Colloid Polym Sci 279: 331–339 (2001)

ORIGINAL CONTRIBUTION

P. Sospedra
M. Espina
M. Castro
S. Corrales
I. Haro
C. Mestres

Miscibility of an acylated hepatitis A synthetic antigen derivative [palmitoyl VP3(110-121)] with lipids: a monolayer study

Received: 26 May 2000
Accepted: 22 September 2000

P. Sospedra · M. Espina · C. Mestres (✉)
Physicochemistry Department
Faculty of Pharmacy
Universitat Barcelona
Av. Joan XXIII s/n
08028 Barcelona, Spain
e-mail: mestres@farmacia.far.ub.es
Fax: +34-93-4035987

M. Castro · S. Corrales
Physicochemistry Department
Faculty of Pharmacy
Universidad Complutense Madrid
Ciudad Universitaria
28040 Madrid, Spain

I. Haro
Department of Peptide & Protein
Chemistry, IIQAB, CSIC
Jordi Girona Salgado
18, 08034 Barcelona, Spain

Abstract Mixed monolayers of an acylated derivative of hepatitis A synthetic peptide VP3(110-121) with neutral, cationic or anionic lipids were spread at the air/water interface. Deviations from ideality as well as thermodynamic values were calculated at different surface pressures using the free-excess energy, the interaction parameter and the enthalpy. The miscibility at the collapse point was also checked. Maximum deviations from ideality were found for mixtures containing the anionic lipid phosphatidylglycerol (PG), and it seems that the monolayer composition is not stable through compression, as the peptide is ejected from the film. Films containing neutral [dipalmitoylphosphatidylcholine (DPPC)] or cationic [stearylamine (SA)] lipids showed more regular behaviour. As the peptide has a net negative charge it is probable that electrostatic interactions are in part responsible of the good miscibility of palmitoyl VP3(110-121) with SA. In order to prepare liposomes containing palmitoyl VP3(110–121), lipids such as SA or DPPC/SA will be a more suitable choice than anionic lipids such as PG.

Key words Hepatitis A · Monolayers · Vaccines · Membrane lipids

Introduction

Chemically synthesized peptides belong to the best-defined vaccine components presently under investigation [1] but they are poorly immunogenic and require the use of adjuvants. To overcome the inherent poor immunogenicity of synthetic peptide antigens several alternatives have been proposed [2, 3]. Among them, the covalent attachment of fatty acid chains has been shown to enhance the immunogenicity of unmodified peptides [4, 5] and their ability to induce the same high affinity to cytotoxic T lymphocytes as the infectious virus [6], bypassing the prerequisite of immunoadjuvants. Recently, many lipopeptides have been synthesized and investigated [7, 8, 9].

Although the underlying mechanism of the increased immunogenicity on peptides by the addition of a lipid tail has not been determined, it is plausible that interaction with, and perhaps through, the cell membrane is important. An understanding of the biophysical nature of the interactions of lipopeptides with model membranes will help to understand the molecular mechanisms involved in the association of lipopeptides with membranes in cells.

In a recent work the physicochemical characterization of the *N*-α-palmitoyl derivative of a dodecapeptide belonging to the VP3 capsid protein of hepatitis A virus (HAV) previously described as a linear epitope of HAV [10] was carried out. To increase the understanding of the interaction of the lipopeptide with lipid membranes, in the present work we report a study of the palmitoylated VP3 peptide miscibility with lipids of different characteristics in monolayers. The effect of the lipopeptide on mixed lipid monolayers has been already studied

[11], and the present work focuses on the miscibility between the peptide and different lipids. A better knowledge of the interactions between the peptide and these lipids will be helpful to understand the behaviour of immunopeptides in biomembranes. All these data can also be useful to prepare immunoliposomes with this peptide in order to increase its immunogenicity.

Experimental

Materials

The synthesis of palmitoyl VP3(110-121) [palmVP3(110-121)], whose structure is given in Fig. 1, has been described already [11]. Dipalmitoylphosphatidylcholine (DPPC), phosphatidylglycerol (PG) and stearylamine (SA) were purchased from Sigma and their purity checked by thin-layer chromatography. Chloroform and methanol (pro analysis) were from Merck.

All experiments were carried out in phosphate buffer solution (PBS) of pH 7.4.

Methods

Peptide characterization

PalmVP3(110-121) was characterized by amino acid analysis, high-pressure liquid chromatography and mass spectrometry and its surface activity determined as detailed in Ref. [11]. Moreover, in the present work, Fourier transform IR (FTIR) and fluorescence spectral data were obtained using a Nicolet 410 spectrophotometer and a Perkin Elmer LS50B fluorimeter, respectively.

The FTIR spectrum was obtained as the average of 120 scans which were collected at 2-cm^{-1} resolution and 25 °C. A liquid flow cell with CaF_2 windows and 60-μm path length spacer was used. The chamber samples were continuously purged with nitrogen and the resultant spectrum was corrected for vapour-phase H_2O absorption by subtraction. The peptide concentration was 2 g/l in D_2O/dimethyl sulfoxide (DMSO). Curve fitting was performed using the Peak Solve program provided by Galactic.

Fluorescence measurements were performed using an excitation wavelength of 295 nm and an experimental temperature of 25 °C. The peptide concentration was 30 μM in H_2O/DMSO.

Compression isotherms

These experiments were performed using a KSV5000 Langmuir film balance, equipped with a Wilhelmy platinum plate and a Teflon trough (surface area 17000 mm^2, volume 1000 cm^3). Monolayers were formed from chloroform solutions or chloroform/methanol (3:1) solution for SA. Lipid–peptide mixed monolayers were spread on the PBS surface from premixed solutions of the components. After the film was spread, 10 min were allowed for solvent evaporation. The monolayers were compressed (symmetrical compression) with an area reduction rate of 60 mm^2/min. Each run was repeated three times, and the reproducibility was ± 0.01 nm^2/molecule. The accuracy of the surface pressure measurements was of 99%. The measurements were carried out at 21 ± 1 °C.

CH_3- $(CH_2)_{14}$-CO- FWRGDLVFDFQV

Fig. 1 PalmVP3(110-121) primary structure

Results

Peptide characterization

Many correlations [12, 13] have been established between the characteristic IR bands of peptides and their conformation. FTIR spectroscopy offers a viable option for the determination of conformations of peptides: the amide I band is especially sensitive to the secondary structure of polypeptides and proteins (Table 1). The structural information is generally extracted by referring to empirical rules on the correspondence between the frequencies of the amide I bands and secondary structure and we have complemented these studies by the second derivative [14, 15]. In these studies information on the structure is extracted from broad envelopes consisting of component bands. As shown in Fig. 2 the FTIR spectrum of VP3(110-121) in D_2O/DMSO exhibits ten bands in the 1600–1700 cm^{-1} region. There is a difference in the relative intensity of the different components. A 30% β structure has been obtained that is in agreement with previous studies [11]; however, according to Table 1 our experimental spectrum clearly shows a higher proportion of unordered structures. Regarding the fluorescence results and comparing them with those obtained when working with nonacylated peptide, a blueshift in the maximum of the tryptophanyl emission was obtained (Fig. 3), thus indicating that the environment surrounding the tryptophanyl residue of the acylated VP3 peptide is perturbed by the fatty acid residue by decreasing the exposition to the solvent.

Pressure–area isotherms of palmVP3(110-121)–lipid mixed monolayers

The ability of palmVP3(110-121), to form stable monolayers has already been described [11]. A compression isotherm obtained when spreading the peptide on a PBS subphase is shown in Fig. 4.

Compression isotherms of DPPC–palmVP3 mixtures are shown in Fig. 5. Mixed monolayers give intermediate curves between DPPC and peptide monolayers,

Table 1 Characteristic IR bands of the amide I VP3(110-121) region

Conformation	Amide frequencies (cm^{-1})
Random coil	~1645
β sheet	~1685, 1630
α helix	~1650

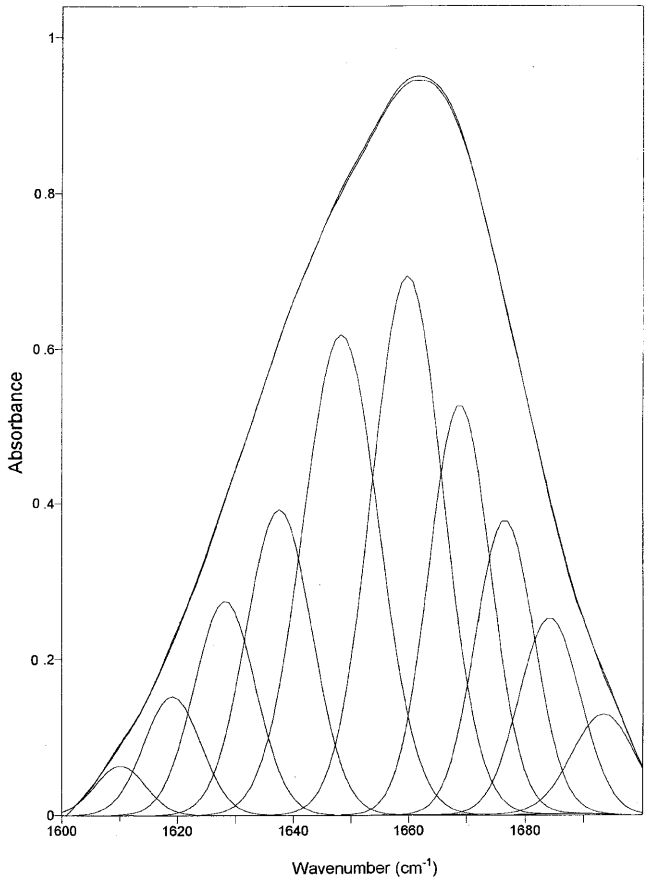

Fig. 2 Fourier transform IR spectrum of palmVP3(110-121) in D_2O/dimethyl sulfoxide

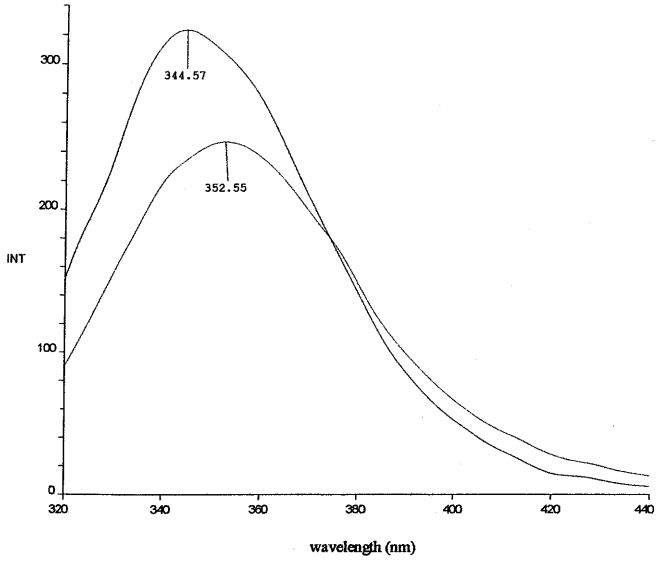

Fig. 3 Fluorescence spectral data for palmVP3(110-121) and VP3(110-121)

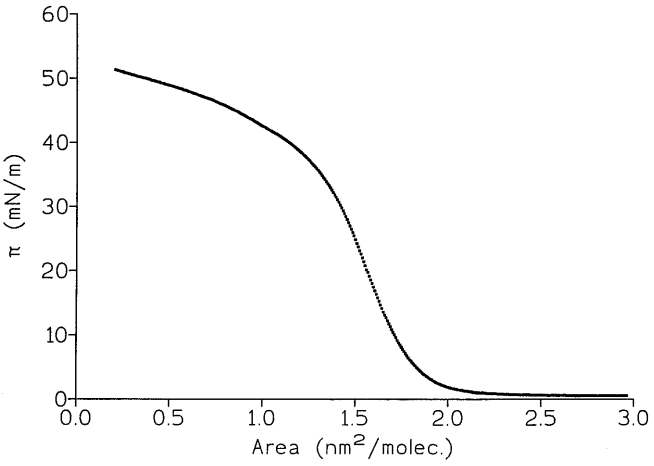

Fig. 4 Surface pressure–area isotherm of palmVP3(110-121). Subphase phosphate buffer solution pH 7.4

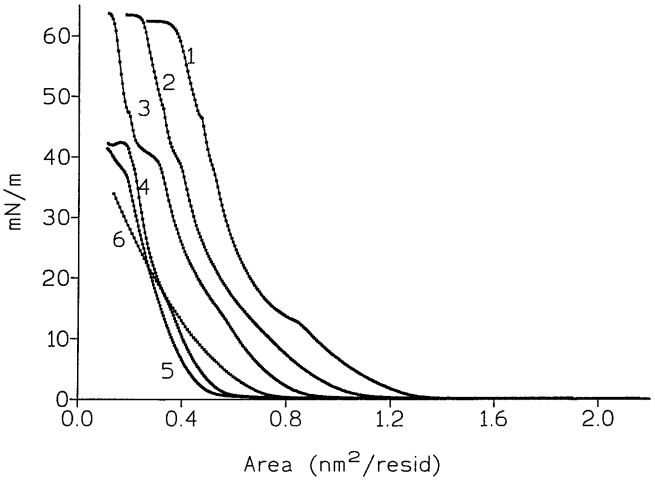

Fig. 5 Surface pressure–area isotherms of *1*: dipalmitoylphosphatidylcholine (*DPPC*); *2*: DPPC/palmVP3(110-121) (0.8:0.2); *3*: DPPC/palmVP3(110-121) (0.6:0.4); *4*: DPPC/palmVP3(110-121) (0.4:0.6); *5*: DPPC/palmVP3(110-121) (0.2:0.8); *6*: palmVP3(110-121)

especially at low peptide compositions. The presence of increasing amounts of peptide results in the disappearance of the well-known DPPC phase transition.

The shape of pressure–area isotherms for mixtures containing 0.2 and 0.4 peptide molar fraction (curves 2 and 3) shows a kink at a surface pressure around 40 mN/m followed by a collapse around 65 mN/m. These two-step collapses can be related to some separation of the components. Mixtures containing 0.6 and 0.8 peptide molar fraction (curves 4 and 5) have a sharp reduction in the collapse pressure. This behaviour has already been described for other peptide mixtures with DPPC [16].

In SA–palmVP3(110-121) mixed monolayers (Fig. 6), the peptide produces fewer variations in the isotherm's

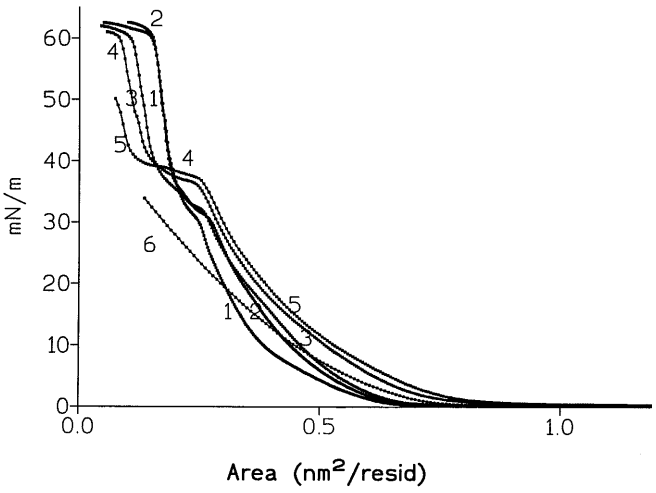

Fig. 6 Surface pressure–area isotherms of *1*: stearylamine (*SA*); *2*: SA/palmVP3(110-121) (0.8:0.2); *3*: SA/palmVP3(110-121) (0.6:0.4); *4*: SA/palmVP3(110-121) (0.4:0.6); *5*: SA/palmVP3(110-121) (0.2:0.8); *6*: palmVP3(110-121)

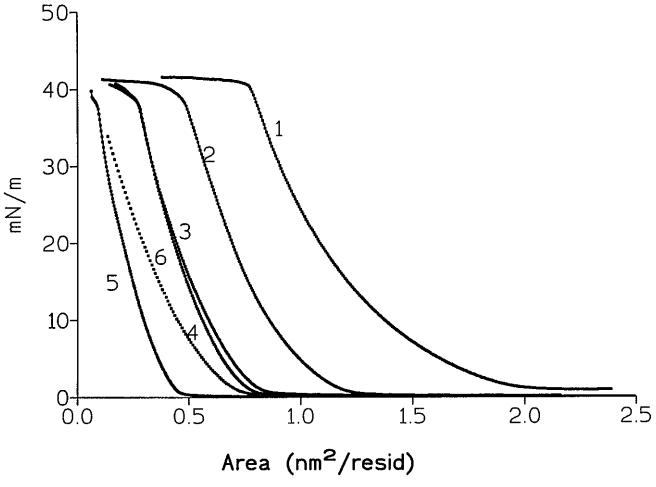

Fig. 7 Surface pressure–area isotherms of *1*: phosphatidylglycerol (PG); *2*: PG/palmVP3(110-121) (0.8:0.2); *3*: PG/PalmVP3(110-121) (0.6:0.4); *4*: PG/palmVP3(110-121) (0.4:0.6); *5*: PG/palmVP3(110-121) (0.2:0.8); *6*: palmVP3(110-121)

shape; however, these variations are irregular depending on the amount of peptide present in the mixture. Changes in the phase transition can be observed and a reduction in the collapse pressure at 0.8 peptide molar fraction.

PG–palmVP3(110-121) monolayers (Fig. 7) showed different behaviour. The differences in area/residue were bigger between the isotherms than in the other cases, but the collapse pressure did not change.

The collapse and transition pressure values for the three systems studied are summarized in Table 2.

Variations in the average area/residue of the mixed films with the peptide mole fraction

The graphs obtained when plotting average area/residue versus molar composition for the three mixtures at different surface pressures are shown in Fig. 8. If the two components are not miscible or are ideally miscible, the plot is a straight line. Deviations from linearity suggest miscibility and some type of molecular interaction between the components.

As can be seen, DPPC and PG, containing monolayers, have negative deviations throughout the mole ratio range. It seems that the peptide has a condensing effect on the monolayer. In DPPC cases, major differences appear when the proportion of peptide increases; for PG, differences are high in all the mixtures assayed. In both cases, deviations are higher at low surface pressures.

SA containing monolayers had completely different behaviour, resulting in positive deviations consistent with an expanding effect.

Plots of excess area of mixing

Another way to check deviations from the ideal behaviour can be done by plotting the excess area of mixing (A_{ex}) as a function of the mole fraction. A_{ex} is defined as the difference between the area/residue occupied by the mixed monolayer at a given surface

Table 2 Collapse and transition pressure values for the monolayers assayed. Dipalmitoylphosphatidylcholine (*DPPC*), phosphatidylglycerol (*PG*), stearylamine (*SA*)

Mole fraction palmVP3 (110–121)	DPPC–palmVP3(110–121)		PG–palmVP3(110–121)		SA–palmVP3(110–121)	
	Transition pressure (mN/m)	Collapse pressure (mN/m)	Transition pressure (mN/m)	Collapse pressure (mN/m)	Transition pressure (mN/m)	Collapse pressure (mN/m)
0	13.5	63.5	–	41.1	30.0	60.0
0.2	38.8	64.1	–	40.0	30.5	60.0
0.4	39.4	64.1	–	37.6	31.7	60.0
0.6	–	42.3	–	37.6	37.6	60.0
0.8	–	42.3	–	37.0	39.4	50.0
1	–	40.0	–	40.0	–	40.0

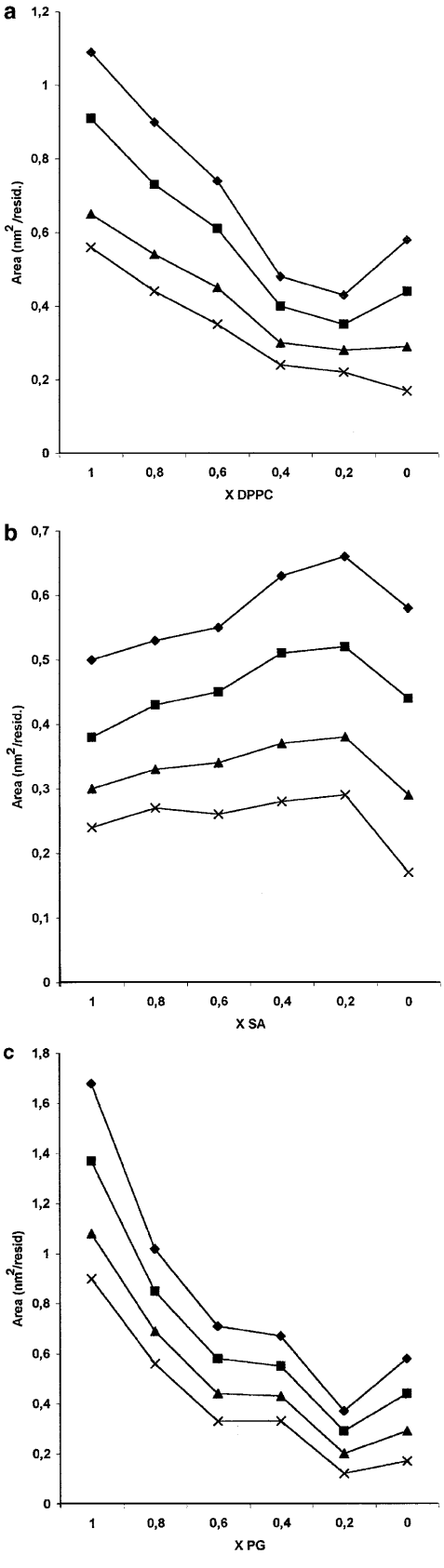

◀

Fig. 8a–c Mean area per "residue" in the lipid/palmVP3(110-121) monolayers as a function of the mole fraction at constant surface pressure: ◆ 5 mN/m, ■ 10 mN/m, ▲ 20 mN/m, × 30 mN/m. **a** DPPC, **b** SA, **c** PG

pressure and the area it would occupy if the components of the mixed film behaved in an ideal manner, and it is calculated by applying Eq. (1).

$$A_{ex} = A_{1,2} - (X_1A_1 + X_2A_2) \ , \tag{1}$$

where $A_{1,2}$ is the molecular area occupied by the mixed monolayer and $(X_1A_1 + X_2A_2)$ is the molecular area occupied by the mixed monolayer, if the components behave in the ideal way. X_1 and X_2 are the mole fractions of components 1 and 2 and A_1 and A_2 are the areas occupied by the pure components [17].

The results obtained are presented in Fig. 9. As expected from the previous plots, it can be seen that for DPPC at 5 mN/m the negative deviations are a maximum. At higher surface pressures (especially at 20–30 mN/m, which are pressures similar to those in bilayers of liposomes and biomembranes) the deviations are so small that practically ideal behaviour can be assumed. PG shows deviations for all pressures, with maximums for 0.4 and 0.8 peptide molar fractions. In the case of SA, the positive deviations are important when the peptide concentration in the monolayer is high.

Thermodynamic parameters

To better quantify the deviations described before, the free energy of mixing ($\Delta G_M{}^{EX}$), the interaction parameter (α) and the enthalpy (ΔH) were calculated.

Calculations were performed following approaches described in Refs. [18, 19, 20, 21], and by applying Eqs. (2), (3) and (4).

$$\Delta G_M^{EX} = \int_{\pi\to 0}^{\pi} A_{1,2}\ d\pi - X_1 \int_{\pi\to 0}^{\pi} A_1\ d\pi - X_2 \int_{\pi\to 0}^{\pi} A_2\ d\pi \ . \tag{2}$$

$A_{1,2}$ is the mean area per residue in the mixed film, A_1 and A_2 are the areas per residue in the pure films and π is the surface pressure. Numerical data were calculated from the compression isotherms according to the mathematical method of Simpson.

$$\alpha = \frac{\Delta G_M^{EX}}{RT\left(X_1X_2^2 + X_1^2X_2\right)} \ , \tag{3}$$

$$\Delta H = \frac{RT\alpha}{Z} \ . \tag{4}$$

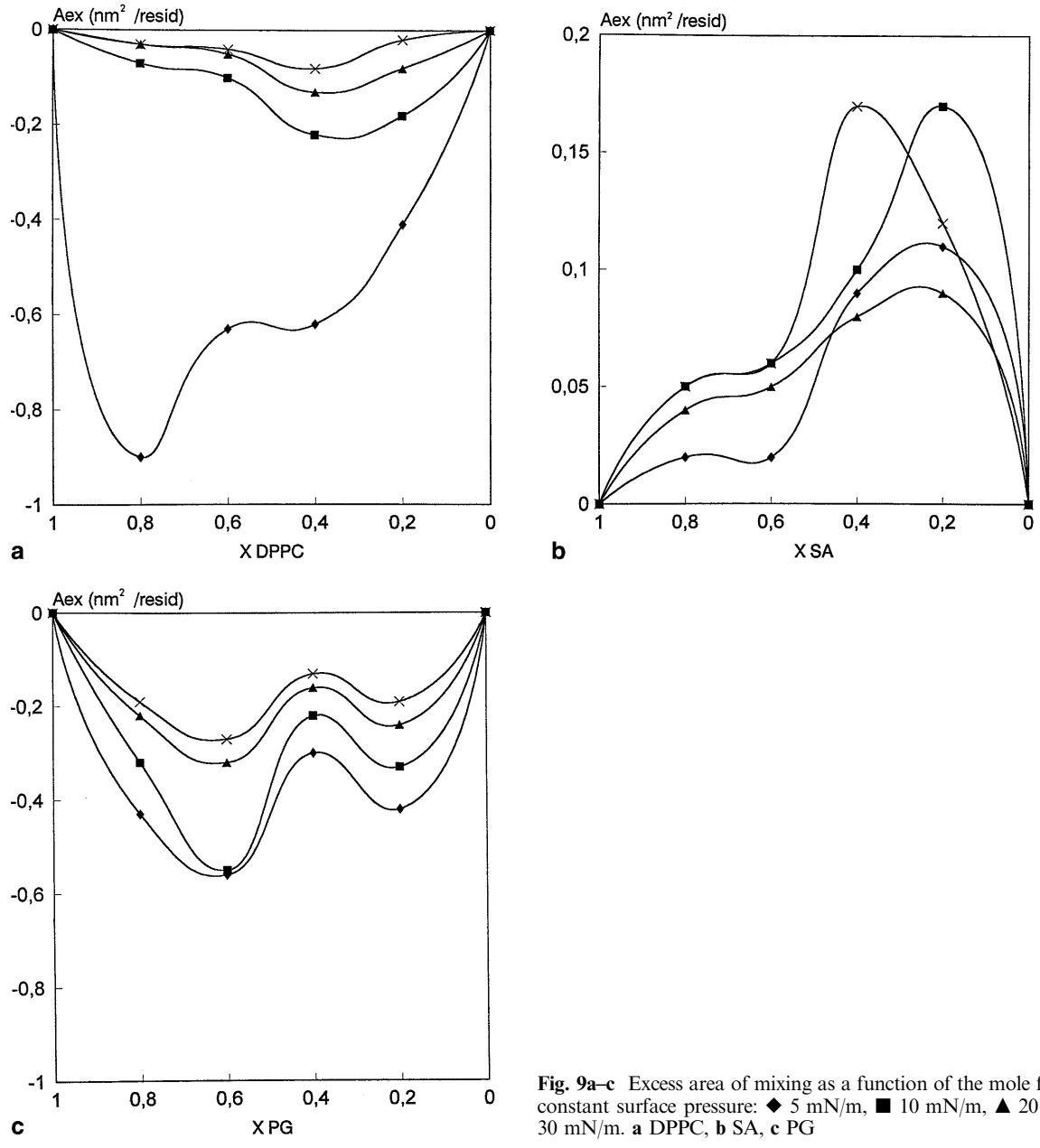

Fig. 9a–c Excess area of mixing as a function of the mole fraction at constant surface pressure: ◆ 5 mN/m, ■ 10 mN/m, ▲ 20 mN/m, × 30 mN/m. **a** DPPC, **b** SA, **c** PG

To calculate the coordination number (Z) the model of Quikenden and Tam [22] was followed, considering that in a closely packed monolayer (collapse), each molecule is surrounded by six neighbours. For lower pressures, Eq. (5) was applied to calculate the packing fraction (PF). This value was used to obtain the corresponding Z, according to the equivalence given by Quickenden and Tam, where $A_{c,m}$ is the area/residue of the mixture at the collapse point and A_m the area/residue of the mixture at the pressure studied.

$$\mathrm{PF} = 0.907\frac{A_{c,m}}{A_m} \tag{5}$$

Tables 3, 4 and 5 show some of the values obtained. On studying these values a low degree of interaction is observed (interaction values of 0). As expected, PG presents higher values, thus suggesting that besides hydrophobic interactions, electrostatic ones are also present.

In some cases it is possible for films at low pressures to be miscible, whereas near the collapse phase separation occurs, so we studied the miscibility at the collapse pressure. When both components are miscible, collapse pressures will vary with composition and the following equation can be applied:

Table 3 Thermodynamic parameters at 10, 20 and 30 mN/m surface pressure for DPPC/palmVP3(110-121)

DPPC	ΔG_M^{EX} (J/mol) Pressure (mN/m)			α Pressure (mN/m)			ΔH (J/mol) Pressure (mN/m)		
	10	20	30	10	20	30	10	20	30
0.8	−3.67	−6.18	−8.10	−0.01	−0.02	−0.02	−11.53	−19.15	−25.45
0.6	−6.06	−9.19	−11.57	−0.01	−0.02	−0.02	−12.62	−19.14	−24.07
0.4	−12.24	−19.52	−24.45	−0.02	−0.03	−0.04	−25.53	−40.67	−50.99
0.2	−10.07	−16.46	−18.30	−0.03	−0.04	−0.05	−31.43	−51.45	−57.22

Table 4 Thermodynamic parameters at 10, 20 and 30 mN/m surface pressure for SA/palmVP3 (110–121)

SA	ΔG_M^{EX} (J/mol) Pressure (mN/m)			α Pressure (mN/m)			ΔH (J/mol) Pressure (mN/m)		
	10	20	30	10	20	30	10	20	30
0.8	0.75	6.47	3.55	0.00	0.02	0.01	2.34	20.27	11.07
0.6	0.96	3.72	4.80	0.00	0.01	0.01	1.96	7.77	10.03
0.4	3.59	7.35	3.28	0.01	0.01	0.01	7.52	15.29	6.81
0.2	4.18	7.98	11.53	0.01	0.02	0.03	13.08	24.99	36.11

Table 5 Thermodynamic parameters at 10, 20 and 30 mN/m surface pressure for PG/palmVP3(110–121)

PG	ΔG_M^{EX} (J/mol) Pressure (mN/m)			α Pressure (mN/m)			ΔH (J/mol) Pressure (mN/m)		
	10	20	30	10	20	30	10	20	30
0.8	−21.86	−31.05	−39.79	−0.06	−0.08	−0.10	−68.34	−97.01	−124.39
0.6	−22.78	−37.99	−50.82	−0.04	−0.06	−0.09	−47.48	−79.16	−105.87
0.4	−15.25	−24.20	−30.89	−0.03	−0.04	−0.05	−31.76	−50.41	−64.37
0.2	−17.93	−30.01	−39.62	−0.03	−0.08	−0.10	−56.01	−93.84	−123.76

$$1 = X_1 e\left(\Pi_{c,m} - \Pi_{c,1}\right) w_1/RT + X_2 e\left(\Pi_{c,m} - \Pi_{c,2}\right) w_2/RT \quad , \tag{6}$$

where X_1 and X_2 are the mole fractions of components 1 and 2 in the monolayer, $\Pi_{c,1}$ and $\Pi_{c,2}$ are collapse pressures of the single components, $\Pi_{c,m}$ is the collapse pressure of the mixed monolayer and w_1 and w_2 are the area/residue of components 1 and 2 at the collapse point.

After substitution of experimental values in these equation, we found that the result is practically 1 (values between 0.98 and 1). This is indicative that at the collapse point the miscibility is ideal.

Changes in the monolayer composition through compression

The following step was to study the stability of the mixtures through compression, calculating monolayer composition when the pressure increases. To this end, the approach described in Refs. [16, 23] was used.

For monolayers of a given composition, the apparent area per lipid molecule, A_1^* was calculated at different surface pressures, dividing the trough area by the number of spread lipid molecules (N_1). The partial "residual" area per amino acid, $\hat{A}_r$, and partial "residual" area per lipid, $\hat{A}_1$, (that represents the contribution of each component to the total area in the mixed monolayer) were evaluated using the method of intercepts used for calculation of partial molar fractions [24]. With these values the excess area per residue, $\Delta A_1 = A_1^* - \hat{A}_1$, equal to the difference between the apparent area and partial "residual" area of the lipid, was calculated as a function of surface pressure.

By dividing ΔA_1 by $\hat{A}_r$, at the same pressure, the number of amino acid residues of palmVP3(110-121) present in the film, $N_r^{calc} = (\Delta A_1/\hat{A}_r)N_r$, ($N_r$ being the number of spread amino acid residues) was obtained. Then the composition of the monolayer $X_r^{calc} = N_r^{calc}/(N_r^{calc} + N_1)$ could be estimated at different surface pressures; these values summarized in Tables 6, 7 and 8.

In all cases, ΔA_1 is positive because the apparent lipid area was higher than the partial lipid area. Apparently, this suggests that the peptide was still incorporated in the monolayer through compression. However in DPPC monolayers containing 0.2 and 0.4 peptide molar fraction consistent values could not be calculated. This could be related to the phase separation pointed out before as well as to the condensing effect produced by

Table 6 Calculated compositions of lipid/palmVP3(110–121) monolayers (X_r^c) as a function of the surface pressure for DPPC

Palm VP3 (110–121) initial mole fraction	PalmVP3(110–121) calculated mole fraction (X_r^c)		
	20 mN/m	30 mN/m	40 mN/m
0.8	0.97	0.98	0.99
0.6	0.88	0.91	0.96
0.4	0.69	0.77	–
0.2	–	–	–

Table 7 Calculated compositions of lipid/palmVP3(110–121) monolayers (X_r^c) as a function of the surface pressure for SA

Palm VP3 (110–121) initial mole fraction	PalmVP3(110–121) calculated mole fraction (X_r^c)			
	20 mN/m	30 mN/m	40 mN/m	50 mN/m
0.8	0.92	0.93	0.96	0.98
0.6	0.60	0.60	0.77	0.86
0.4	0.20	0.19	0.37	0.45
0.2	0.03	0.02	0.06	0.05

Table 8 Calculated compositions of lipid/palmVP3(110–121) monolayers (X_r^c) as a function of the surface pressure for PG

Palm VP3 (110–121) initial mole fraction	PalmVP3(110–121) calculated mole fraction (X_r^c)		
	20 mN/m	30 mN/m	40 mN/m
0.8	0.98	0.92	0.99
0.6	0.96	0.99	–
0.4	–	–	–
0.2	–	–	–

the peptide, which can be related to a reduction in the monolayer elasticity for these mixtures as can be seen in Fig. 10. It seems that even for $\Delta A_1 > 0$, which suggests the possible incorporation of the peptide into the monolayer, some molecules are ejected from it, although it was not possible to quantify this.

A similar problem arose with PG mixtures. In this case consistent values of X_r^{calc} could only be calculated for very few mixtures.

As expected from the previous results, SA had more regular behaviour. As can be deduced from the results obtained, the expanding effect is consistent with the fact that the peptide remains in the monolayer through compression, even at high pressures near the collapse.

Discussion

The results obtained show that SA–palmVP3(110-121) mixtures are more stable through compression, with

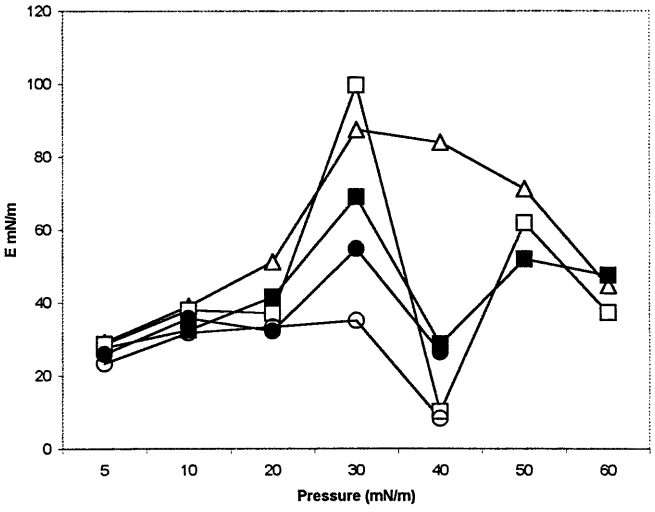

Fig. 10 Surface elasticity of DPPC/palmVP3(110-121) monolayers as a function of the surface pressure. Δ DPPC, ■ DPPC/palmVP3(110-121) (0.8:0.2) □ DPPC/palmVP3(110-121) (0.6:0.4) ● DPPC/palmVP3(110-121) (0.4:0.6), ○ DPPC/palmVP3(110-121) (0.2:0.8)

very low interaction energies, especially for monolayers with high peptide composition. It seems that besides hydrophobic interactions usually present in these systems, electrostatic forces also play an important role. The fact that SA is a cationic lipid and that palmVP3(110-121) has a net negative charge may be responsible of the higher stability of these mixtures owing to the establishment of attractive electrostatic interactions. However, monolayers with high lipid composition present lower X_r^{calc} values, which suggests that the incorporation of the peptide into the monolayer is enhanced when SA molar fractions are around 0.2–0.4.

Interactions with an anionic lipid such as PG are more difficult to interpret. It is clear that a condensing effect is produced but the deviations do not correlate very well with the regular behaviour found at the collapse. When trying to calculate X_r^{calc}, it was clear that the mixture composition was not stable through compression and that some of the peptide was squeezed out of the monolayer. Previous results seemed to suggest that miscibility between PG and palmVP3(110-121) was good (similar collapse pressure for all the mixtures); however, palmVP3(110-121) has a stronger condensing effect on the monolayer than with DPPC and may thus lead to the exclusion of the peptide from the monolayer. Repulsive interactions between lipid and peptide could be responsible for this behaviour.

DPPC mixtures have different behaviour depending on the composition. Monolayers with peptide molar fractions of 0.2 and 0.4 showed a kink around 40 mN/m that correlates with a reduction in the elasticity and a possible phase separation or rearrangement due to peptide ejection from the monolayer or a change in the

peptide conformation. The monolayers with peptide molar fractions of 0.6 and 0.8 had a sharp reduction in the collapse pressure, but no loss of peptide from the monolayer was detected.

In previous work in our laboratory [25], the parent peptide VP3(110-121) showed a similar pattern, with SA containing monolayers being the most stable.

Conclusions

- PalmVP3(110-121) mixtures with SA, DPPC and PG present different patterns of behaviour, even though deviations obtained are not particularly great.
- In the interactions between palmVP3(110-121) and these lipids both hydrophobic and electrostatic interactions play an important role.
- The mixtures with SA are more predictable and stable.
- In order to prepare liposomes containing palmVP3(110-121) as vaccines, cationic lipids seem more suitable.
- Derivatization of VP3(110-121) with palimitic acid does not change significantly its miscibility with DPPC, PG and SA.

Acknowledgements This work was supported by grant PB-96-0596-C02-01 from DGICYT, Spain, and a predoctoral CIRIT grant (1997 FI000073) awarded to P.S.

References

1. Arnon R, Horwitz RJ (1992) Curr Opin Immunol 4:449
2. Del Giudice G (1992) Curr Opin Immunol 4:454–459
3. Tam JP (1996) J Immunol Methods 196:17–32
4. Sela M (1980) In: Larralde C, Wills K, Ortiz-Ortiz L, Sela M (eds) Molecules, cells and parasites in immunology. Academic, New York, pp 215–228
5. Hopp T (1984) Mol Immunol 21:13–16
6. Volpina OM, Yarov AV, Zhmak MN, Kuprianova MA, Chepurkin AV, Toloknov AS, Ivanov VT (1996) Vaccine 14:1375–1380
7. Deres K, Schild H, Wiesmuller KH, Jung G, Rammensee HG (1989) Nature 342:561–564
8. Deprez B, Sauzet JP, Boutillon C, Martinon F, Tartar A, Sergheraert C, Guillet JG, Gomard E, Grass-Masse H (1996) Vaccine 14:375–382
9. Laczko I, Hollsi M, Vass E, Toth GK (1998) Biochem Biophys Res Commun 249:213–217
10. Bosch A, Gonzalez-Dankaart JF, Haro I, Gajardo R, Pérez JA, Pintó RM (1998) J Med Virol 54: 95–102
11. Sospedra P, Haro I, Alsina MA, Reig F, Mestres C (1999) Mater Sci Eng C 8–9:543–549
12. Payne KJ, Veis A (1988) Biopolymers 27:1749–1760
13. Dong A, Huang P, Caughey WS (1990) Biochemistry 29:3303–3308
14. Byler DM, Susi H (1986) Biopolymers 15:607–625
15. Surewicz WZ, Mantzch HH, Capman D (1993) Biochemistry 32:389–394
16. Taneva S, Panaiotov I (1984) Colloid Surf 10:101–111
17. Seoane P, Miñones J, Conde O, Casas M, Iribarnegaray E (1998) Biochim Biophys Acta 1375:73–83
18. Goodrich FC (1957) Proceedings of the 11th International Congress on Surface Activity. Butterworths, London
19. Pagano RE, Gershfeld NL (1972) J Colloid Interface Sci 41:311
20. Joos P, Demel RA (1969) Biochim Biophys Acta 183:447–457
21. Queraltó A, Aznarez MD, Castro RM, Otero E (1980) An R Acad Farm 46:101–116
22. Quickenden TI, Tam GK (1974) J Colloid Interface Sci 48:382
23. Taneva S, Keough KMW (1994) Biophys J 66:1137–1148
24. Moore W (1962) Physical chemistry. Prentice-Hall, Englewood Cliffs, p 844
25. Sospedra P, Alsina MA, Espina M, Reig F, Haro I, Mestres C (2000) J Colloid Interface Sci 221:230–235